

Cumulative damage-based inelastic cyclic demand spectrum

S. K. Kunnath^{*,†} and Y. H. Chai

Department of Civil and Environmental Engineering, University of California, Davis, CA 95616, U.S.A.

SUMMARY

The estimation of cyclic deformation demand resulting from earthquake loads is crucial to the core objective of performance-based design if the damage and residual capacity of the system following a seismic event needs to be evaluated. A simplified procedure to develop the cyclic demand spectrum for use in preliminary seismic evaluation and design is proposed in this paper. The methodology is based on estimating the number of equivalent cycles at a specified ductility. The cyclic demand spectrum is then determined using well-established relationships between seismic input energy and dissipated hysteretic energy. An interesting feature of the proposed procedure is the incorporation of a design spectrum into the proposed procedure. It is demonstrated that the force–deformation characteristics of the system, the ductility-based force-reduction factor R_μ , and the ground motion characteristics play a significant role in the cyclic demand imposed on a structure during severe earthquakes. Current design philosophy which is primarily based on peak response amplitude considers cyclic degradation only in an implicit manner through detailing requirements based on observed experimental testing. Findings from this study indicate that cumulative effects are important for certain structures, classified in this study by the initial fundamental period, and should be incorporated into the design process. Copyright © 2003 John Wiley & Sons, Ltd.

KEY WORDS: cumulative seismic damage; input energy; hysteretic energy; low-cycle fatigue

INTRODUCTION

Current provisions for seismic design are based on peak demands without explicit consideration of cumulative damage effects resulting from inelastic cyclic response. The deformation demands imposed on a structural component by an earthquake ground motion are cyclic in nature and the associated effects of cumulative damage can play a significant role in altering the seismic resistance of the system. As pointed out in a recent paper by Malhotra [1], the peak amplitude by itself is not an adequate measure of the potential damage of a ground motion and hence not a good predictor of system performance because the strength, stiffness

*Correspondence to: S. K. Kunnath, Department of Civil and Environmental Engineering, University of California, Davis, CA 95616, U.S.A.

†E-mail: skkunnath@ucdavis.edu

Contract/grant sponsor: National Science Foundation; contract/grant number: CMS-0296210

Received 31 March 2003

Revised 26 July 2003

Accepted 23 September 2003

and energy-dissipation capacity of the structure are inherently dependent on the number of inelastic load cycles. The proposed formulations can be viewed as an extension of Malhotra's work wherein several critical design variables ranging from ground motion characteristics to system response parameters have now been incorporated into the methodology.

The estimation of seismic input energy into a structure has been the subject of numerous investigations [2–4]. It is well established that the input energy to a structure near the predominant period of the ground motion is a stable quantity, which may be predicted with reasonable accuracy from ground motion parameters. The amount of hysteretic energy to be dissipated may be estimated as a fraction of the total input energy. Several semi-empirical expressions have been proposed [4–6] to evaluate the contribution of hysteretic energy in dissipating the overall input energy. Unlike the input energy, however, the amount of the hysteretic energy dissipated by the structure depends on the properties of the structure including the period and strength of the structure. In the procedure set forth in this paper, it is assumed that a reliable expression relating the input energy to the energy dissipated by system yielding is available. Once such an expression is selected, the rest of the procedure is relatively straightforward. The objective of this paper is to define a hysteretic energy-based spectrum for the number of inelastic load cycles that a structure may experience in order to characterize the damage potential of the earthquake ground motion. To this end, it is necessary to incorporate standard design procedures, such as the use of an inelastic design spectrum and associated force-reduction factor as characterized by the $R_{\mu}-\mu_c-T$ relations.

RELATIONSHIP BETWEEN CYCLIC DEMAND AND DISSIPATED ENERGY

Of particular interest in the development of a demand spectrum are earthquake forces that cause elements in the structural system to deform beyond the elastic limit, thereby resulting in the dissipation of energy. Since the dissipation of energy in a structural system can be treated as a critical measure of the seismic resistance of the system, it is important to establish a simple relationship that translates dissipated energy into a cyclic demand parameter.

Non-linear force–deformation behavior in a structural element is a function of numerous parameters ranging from material type (steel, reinforced concrete, etc.) to internal force interaction to detailing. In the context of the present formulation, it is essential to begin with simple definitions and then extend them to more complex behavior patterns. A commonly used idealization of the non-linear behavior is the elastic perfectly-plastic behavior shown in Figure 1. Assuming yield forces in the positive and negative direction to be V_y^+ and V_y^- , respectively, and corresponding yield displacements u_y^+ and u_y^- , consider the case of a simple system subjected to one full cycle of loading to peak displacements of u_{\max}^+ and u_{\max}^- . In this case, the energy dissipated by the yielding element per cycle is:

$$E_c = (V_y^+ + V_y^-) \{ (u_{\max}^+ - u_y^+) + (u_{\max}^- - u_y^-) \} \quad (1)$$

If symmetric behavior is assumed i.e., $V_y^+ = V_y^- = V_y$ and $u_y^+ = u_y^- = u_y$, and if equal peak displacements of $u_{\max}^+ = u_{\max}^- = u_{\max}$ are imposed in the two directions, Equation (1) can be rewritten as:

$$E_c = 4V_y u_{\max} (1 - 1/\mu_c) \quad (2)$$

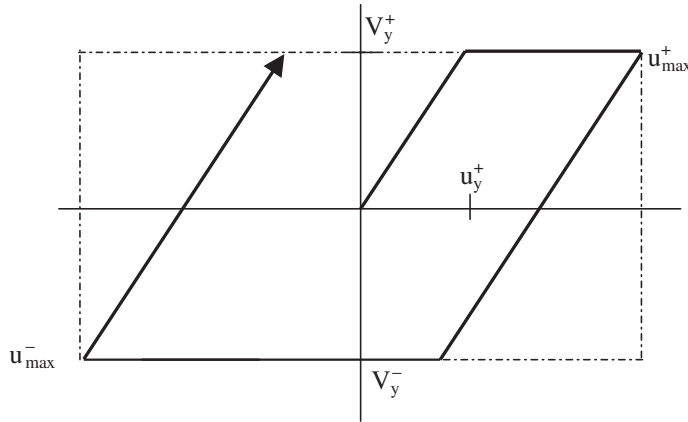


Figure 1. Idealized force–deformation behavior.

where $\mu_c = u_{max}/u_y$ = cyclic displacement ductility factor. The above expression can be generalized as follows:

$$E_c = \alpha_h 4V_y u_{max} \tag{3}$$

where α_h is an energy shape factor that depends on both the ductility and the shape of the hysteresis loops. For example, in the case of an elastic-plastic system depicted in Figure 1, the energy shape factor $\alpha_h = (1 - 1/\mu)$. For more complex shapes which incorporate degradation and pinching effects, the estimation of this factor is less obvious and will be discussed later in this paper.

In the formulation leading to Equation (3), only a single hysteretic loop at ductility μ_c was considered. For a non-degrading system subjected to N_f full cycles at the same ductility, the total energy dissipated is the product of N_f and E_c . If u_{max} is rewritten in terms of the ductility demand such that $u_{max} = \mu_c u_y$, then the following expression between the number of inelastic cycles and dissipated hysteretic energy can be derived:

$$N_f = \frac{E_h}{4\alpha_h \mu_c V_y u_y} \tag{4}$$

The above expression essentially converts the dissipated energy into an equivalent number of cycles at a given cyclic displacement ductility factor. The yield strength of the system is generally a well-defined quantity and may be related to the elastic seismic force demand through the commonly used force-reduction factor. The yield displacement term in Equation (4), however, needs to be eliminated from the equation since it is necessary to carry out an analysis of the structure to estimate this parameter. This can be accomplished by associating the yield displacement with the stiffness of the system which in turn is related to the fundamental period as follows:

$$\omega^2 = k/m \Rightarrow \frac{V_y/u_y}{m} \tag{5}$$

where ω = circular frequency of the fundamental mode, and m and k are the seismic mass and lateral stiffness of the system, respectively, which leads to:

$$u_y = \frac{V_y T^2}{4m\pi^2} \quad (6)$$

where T = fundamental period of the structure. Substituting Equation (6) into Equation (4) results in:

$$N_f = \frac{m\pi^2 E_h}{\alpha_h \mu_c (V_y T)^2} \quad (7)$$

The above expression provides a convenient relationship between dissipated energy and the equivalent number of inelastic cycles, which characterizes the cumulative energy-based cyclic demand in terms of fundamental design quantities, V_y and T . To complete the energy-cyclic demand relationship in a format that can be used later in the development of the demand spectra, it is necessary to eliminate the design base shear force and replace it with a description of the design spectra which also incorporates the force-reduction factor. To do this, consider the definition of design base shear force, V_y :

$$V_y = \frac{mS_a}{R_\mu} \quad (8)$$

where R_μ is the force-reduction factor and S_a is the design spectral acceleration. Substitution of Equation (8) into Equation (7) yields:

$$N_f = \left(\frac{E_h}{m} \right) \frac{\pi^2}{\mu_c \alpha_h} \left(\frac{R_\mu}{TS_a} \right)^2 \quad (9)$$

APPLICATION IN SEISMIC EVALUATION AND DESIGN

The expression given in Equation (9) is a measure of the cyclic demand given the following parameters: a measure of the dissipated hysteretic energy of the structure for the design event defined by E_h/m ; the design ductility μ_c ; the hysteresis shape factor α_h ; the ductility-based force-reduction factor R_μ and the spectral acceleration of the design earthquake at the fundamental period of the structure. The application of Equation (9) to compute the number of cycles for a site-specific ground motion is relatively straightforward and will be illustrated in the validation exercise to be discussed in the next section. However, to determine the cyclic demand in a seismic design context it is necessary to establish a set of relationships that make it possible for each of the parameters to be evaluated using structural response characteristics such as ductility, dissipated energy, etc. and general ground motion parameters such as PGA and PGV. In the present paper a set of empirical equations, taken directly or modified from formulations available in the literature, is used to achieve these relationships. The purpose here is to demonstrate the methodology rather than arrive at final design equations for general structural systems. Some of the empirical equations have been calibrated to accommodate the proposed procedure without the benefit of a large database. Hence, it is important to view the relationships described in the following sections as conceptual starting points which can be improved as new calibrated data becomes available.

Elastic seismic design spectrum

The design earthquake is commonly described in traditional seismic design by means of an elastic response spectrum. To this end, the design spectral acceleration S_a in Equation (9) can be related to the peak ground acceleration $\ddot{x}_{g,max}$ through a period-dependent amplification factor Ω_a as follows:

$$S_a = \Omega_a \ddot{x}_{g,max} \tag{10}$$

In this paper, the description of the amplification factor which provides the elastic response acceleration spectrum is based on the formulation proposed by Vidic *et al.* [7] and modified by Chai *et al.* [8]. The variation of Ω_a with period T is as follows:

$$\Omega_a = \begin{cases} 1.0 + 2.5(c_a - 1)T/T_c & 0 < T \leq 0.4T_c \\ c_a & 0.4T_c < T \leq T_c \\ 2\pi c_v (\dot{x}_{g,max}) / (\ddot{x}_{g,max} T) & T > T_c \end{cases} \tag{11}$$

$$T_c = 2\pi \frac{c_v \dot{x}_{g,max}}{c_a \ddot{x}_{g,max}} \tag{12}$$

where the coefficient c_a is the ratio of the elastic spectral acceleration to peak ground acceleration in the short-period range and c_v is the ratio of the spectral velocity to the peak ground velocity in the velocity-controlled range of the response spectrum; and the coefficients $\dot{x}_{g,max}$ and $\ddot{x}_{g,max}$ are the peak ground velocity and acceleration, respectively. A value of $c_a = 2.5$ and $c_v = 2.0$ was used by Chai *et al.* [8]. The coefficients c_a and c_v should not be confused with those used in the Uniform Building Code. The parameter T_c in Equation (12) corresponds to the characteristic period of the ground motion and has been taken from the expression proposed by Vidic *et al.* [7]. The predominant period T_c is assumed to coincide with the period at which the peak value of the input energy occurs. The motivation for this description of the spectral content results from the fact that the ratio of peak ground acceleration to peak ground velocity (a/v) is known to be a good parameter for characterizing the frequency content of the ground motion. Additionally, a low a/v ratio, for example, characterizes a soft-soil site while a high a/v ratio characterizes a firm or rock-soil site. These effects are illustrated in Figure 2, which plots the variation of the elastic amplification factor Ω_a as defined by Equation (11). Note that the influence of soil type is reflected not in the amplitude but in the spectral shape. The peak amplification covers a larger period range for low a/v values, as is to be expected for soft soil conditions.

Inelastic response spectrum and force reduction factor: $R_{\mu-\mu_c}-T$ relationship

The response spectrum discussed in the previous section considers an elastic response only. In order to extend its application to the non-linear range, seismic design codes commonly employ the use of a force-reduction factor. Though code-based force-reduction factors R consider more than simply the ductility demand in developing these factors (the effects of over-strength and redundancy also play an important role), the present study limits the application of the reduction factor to ductility-based effects. Hence, the terminology R_{μ} is employed. Numerous

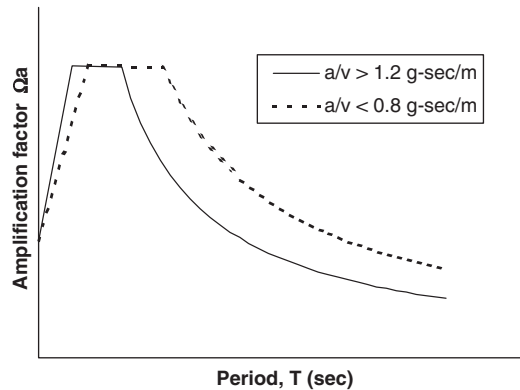


Figure 2. Acceleration amplification factor for elastic response.

expressions for the force-reduction factor as a function of period and ductility can be found in the literature. In order to remain consistent with the definition of the elastic acceleration amplification factor (Equation (9)), the following expression proposed by Vidic *et al.* [7] is used:

$$R_{\mu} = \begin{cases} (\mu_c - 1)T/T_0 + 1 & T \leq T_0 \\ \mu_c & T > T_0 \end{cases} \quad (13)$$

where

$$T_0 = 0.65T_c(\mu_c)^{0.3} \quad (14)$$

In the above expression, the transition period T_0 is related to the characteristic period T_c which has been defined previously in Equation (12). It should be noted that the transition period T_0 in Equation (14) has been calibrated for a stiffness-degrading model, which is appropriate for reinforced concrete members. The dependence of R_{μ} on the characteristic period implies its relationship to site effects. Figure 3 plots the variation of the ductility-based force-reduction factor R_{μ} for the same high and low a/v values used to generate the acceleration amplification curve in Figure 2. These plots confirm our intuitive understanding of the force-reduction factor, which are relatively constant (and converges to the cyclic ductility demand parameter, μ_c) for long-period systems and decreases rather abruptly to unity for short, stiff structures.

Finally, it is reiterated that the definitions and expressions used in arriving at $R_{\mu}-\mu_c-T$ relationships and the resulting inelastic response spectrum do not consider components of over-strength and redundancy that are known to influence the inelastic response of structures. However, these factors can be incorporated into the proposed methodology for MDOF systems.

Seismic energy demand

It has been shown [5] that for an elastic undamped single-degree-of-freedom system, the Fourier amplitude spectrum of the ground acceleration $|F(\omega)|$ is equal to the equivalent input

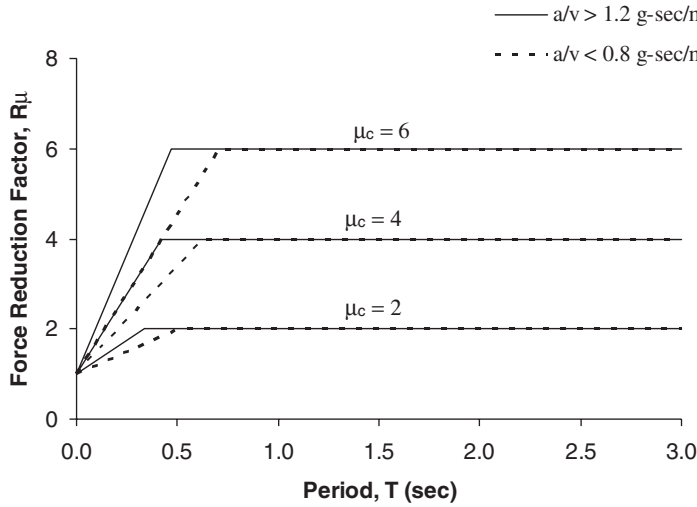


Figure 3. $R-\mu-T$ relationship used in formulation.

energy velocity, v_e :

$$v_e = |F(\omega)| = \left(\frac{2E_I}{m} \right)^{0.5} \tag{15}$$

where m is the mass of the system and E_I is the input earthquake energy. A familiar approach in energy-based design [6] is to assume that the equivalent input energy velocity is a product of the peak ground velocity, $\dot{x}_{g,max}$ and an amplification factor, Ω_v :

$$v_e = \Omega_v(\dot{x}_{g,max}) \tag{16}$$

The amplification factor for the input energy, as given in Equation (16), was found to have a significant influence on the computed cyclic demand. Hence, a separate study was carried out to calibrate this parameter. A set of ground motions (Table I) with varying characteristic periods and varying a/v ratios was evaluated. Typical results obtained from the calibration study are displayed in Figure 4. It was established that the variation of the input energy followed a roughly parabolic path up to the characteristic period (corresponding to the peak input energy) followed by a gradual decay. Based on these results, the following relationship is proposed to characterize the variation of the amplification factor Ω_v :

$$\Omega_v = \begin{cases} \Omega_v^* \left(\frac{2T}{T_c} - \left[\frac{T}{T_c} \right]^2 \right); & T < T_c \\ \Omega_v^* \left[\frac{T}{T_c} \right]^{-\lambda}; & T > T_c \end{cases} \tag{17}$$

Table I. Characteristics of earthquakes used in validation studies.

Earthquake	Station	PGA (g)	PGV (m/s)	PGD (m)	a/v (g/ms^{-1})	t_d
Kobe 1995	Takatori	0.61	1.27	0.36	0.48	13.36
Kobe 1995	Takatori	0.62	1.21	0.33	0.51	11.94
Imperial Valley 1940	El Centro	0.22	0.30	0.23	0.72	25.95
Northridge 1994	Castaic	0.51	0.52	0.15	0.99	10.58
Imperial Valley 1940	El Centro	0.31	0.30	0.13	1.05	26.11
Northridge 1994	Castaic	0.57	0.52	0.09	1.09	11.10
Fruili 1976	San Rocco	0.06	0.05	0.01	1.24	7.04
Loma Prieta 1989	Gilroy	0.41	0.32	0.06	1.30	8.54
Loma Prieta 1989	Gilroy	0.47	0.34	0.08	1.40	5.69
Fruili 1976	San Rocco	0.13	0.08	0.02	1.77	7.00
Fruili-02 1976	Forgario Cornino	0.21	0.10	0.02	2.19	6.53
Fruili-02 1976	Forgario Cornino	0.26	0.09	0.01	2.81	6.49
Mexico City 1985 ^a	SCT	0.10	0.38	1.24	0.26	30.00
Chile 1985 ^a	Llolleo	0.45	0.13	0.06	3.32	30.00

^aOnly a portion of these records were used in the simulations, hence the strong motion duration indicated here does not reflect the actual earthquake duration.

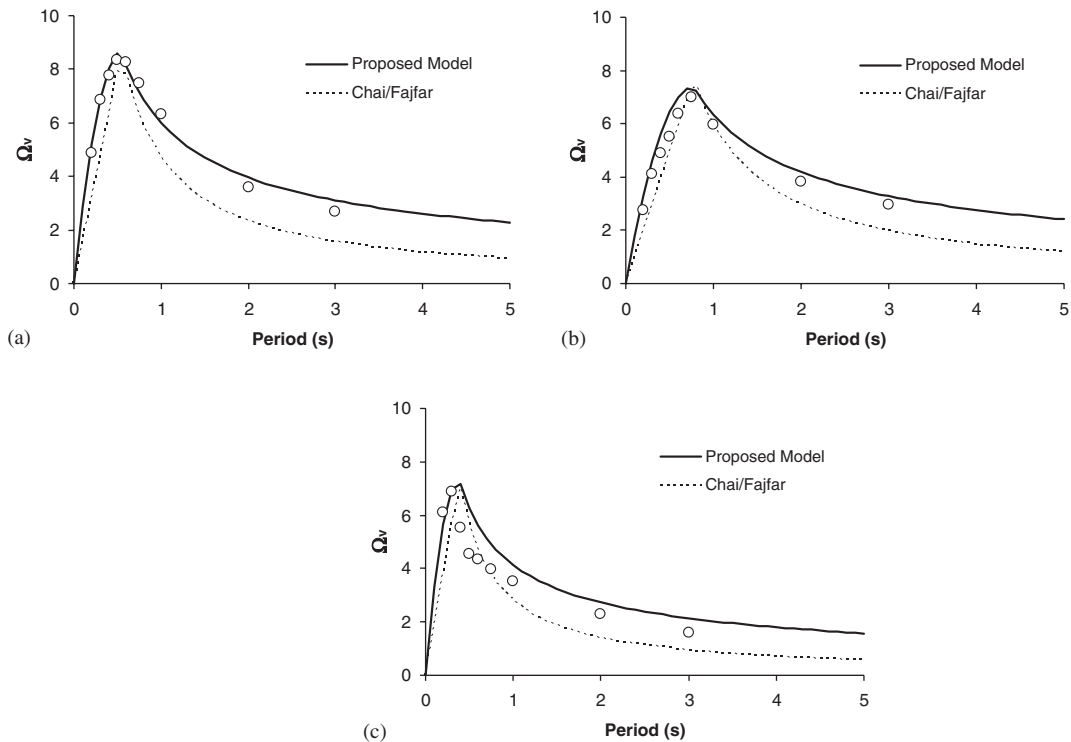


Figure 4. Calibration of the amplification factor for input energy: (a) Northridge 1994, Castaic-360; $a/v=1.0$; (b) Kobe 1995, Takatori; $a/v=0.5$; and (c) Loma Prieta 1989, Gilroy; $a/v=1.4$.

and

$$\Omega_v^* = \frac{0.25(\ddot{x}_{g,\max})}{\dot{x}_{g,\max}} \sqrt{t_d T_c} \sqrt{\frac{\lambda + 0.5}{2\lambda + 2}} \tag{18}$$

where Ω_v^* is the peak amplification factor for the input energy spectrum, λ is a parameter that characterizes the spectral shape of the input energy spectrum for periods longer than the predominant period of the ground motion, and t_d is the duration for the strong motion phase of the ground motion. The strong motion duration used in the above equation is based on the following definition by Trifunac and Brady [9]:

$$t_d = t_{0.95} - t_{0.05} \tag{18a}$$

where $t_{0.05}$ and $t_{0.95}$ denote the time at 5% and 95% of the Arias intensity I_A which is given by:

$$I_A = \frac{\pi}{2g} \int_0^{t_0} \dot{x}_g^2 dt \tag{18b}$$

The above definition of duration is commonly used for characterizing the input energy of earthquake ground motions. However, this definition of duration does not account for ‘silent gaps’ in long records and is also not appropriate for near-field motions characterized by velocity or displacement pulses. Since the Arias intensity is based on acceleration history, the application of the definition given by Equation (18a) may not be valid for very long period structures. These limitations should be noted when interpreting the results presented later in this paper. Finally, a value of $\lambda = 0.5$ was found to be more appropriate for the earthquake ground motions considered in this study than the value of $\lambda = 1$ suggested by Chai and Fajfar [6].

The input energy per unit mass, i.e. Equation (15), is more conveniently expressed in the following form:

$$\frac{E_l}{m} = 0.5v_c^2 \tag{19}$$

The hysteretic energy to be dissipated by the system can be expressed as a fraction α of the total seismic input energy as follows:

$$\frac{E_h}{m} = \alpha \frac{E_l}{m} \tag{20}$$

Various empirical equations have been suggested by a number of researchers to estimate the ratio α . Here, the expression proposed by Fajfar and Vidic [3] is used:

$$\alpha = 1.13 \frac{(\mu_c - 1)^{0.82}}{\mu_c} \tag{21}$$

The constants which appear in the above equation were calibrated by Chai *et al.* [8] using a stiffness degrading model and four different earthquake ground motions.

Influence of hysteretic shape on energy demand

The expression (Equation (9)) which defines the equivalent number of inelastic cycles at design ductility factor μ_c is dependent upon the dissipated hysteretic energy per unit mass, the force-reduction factor, the natural period of the structure and the force–deformation characteristics of the system. All of these variables have been completely defined with the exception of the hysteresis loop shape factor, α_h . A parametric study was carried out to evaluate the effect of different hysteresis shapes on the dissipated energy. A pinched smooth hysteresis model based on the Baber–Noori formulation [10] but extended by Kunnath *et al.* [11] to include stiffness degradation and strength deterioration was used in the evaluation. Three model types were considered: bilinear, to represent non-degrading systems such as steel; degrading, to represent moderate degrading effects in structures with well-detailed concrete members; and pinched-degrading, to represent severely degrading systems with very limited energy dissipation capacity. Figure 5 displays typical loop shapes generated by these hysteretic models. Next, the hysteresis shape factor, α_h , was computed for each of the three models as a function of the number of cycles. The results of the analyses are shown in Figure 6 for the three hysteretic models. The shape factor exhibits minimal variation for bilinear systems. However, the variation of the shape factor for degrading systems is considerable with increasing number of cycles. While it may be argued that it is necessary to derive an expression for the shape factor as a function of ductility and the number of cycles, a simple approach was used in this study to avoid the complexity of transforming the methodology into a non-linear problem requiring an iterative solution. The following constant values were used:

$$\begin{aligned}\alpha_h &= 0.75 \text{ for bilinear systems} \\ \alpha_h &= 0.50 \text{ for degrading systems} \\ \alpha_h &= 0.25 \text{ for pinched, degrading systems}\end{aligned}$$

The results obtained with these constant values are expected to be a reasonable approximation of the true demands which offer an insight into the concept of cyclic demand and the factors that influence the equivalent number of cycles.

VALIDATION OF PROPOSED FORMULATION

It is well known that fatigue-life relationships for most structural materials typically take the following modified form of the Coffin [12]–Manson [13] relationship:

$$2N_f = c_1(\Delta)^{c_2} \quad (22)$$

in which $2N_f$ is the number of constant-amplitude half-cycles (or the number of reversals) to failure, c_1 and c_2 are material constants established from experimental fatigue testing and Δ is a measure of deformation (total strain, plastic strain, drift, displacement, etc.). A fatigue-life model of the form of Equation (22) and a cumulative damage model (which in the context of this paper is defined using Miner's hypothesis [14]) provide a rational basis to develop a cycle-counting procedure for arbitrary deformation histories. Details of the process outlined in the next section also serve to clarify the validation exercise.

The methodology proposed in this paper is validated using seismic simulations of a reinforced concrete bridge model, comprising a single pier and deck structure, which is amenable

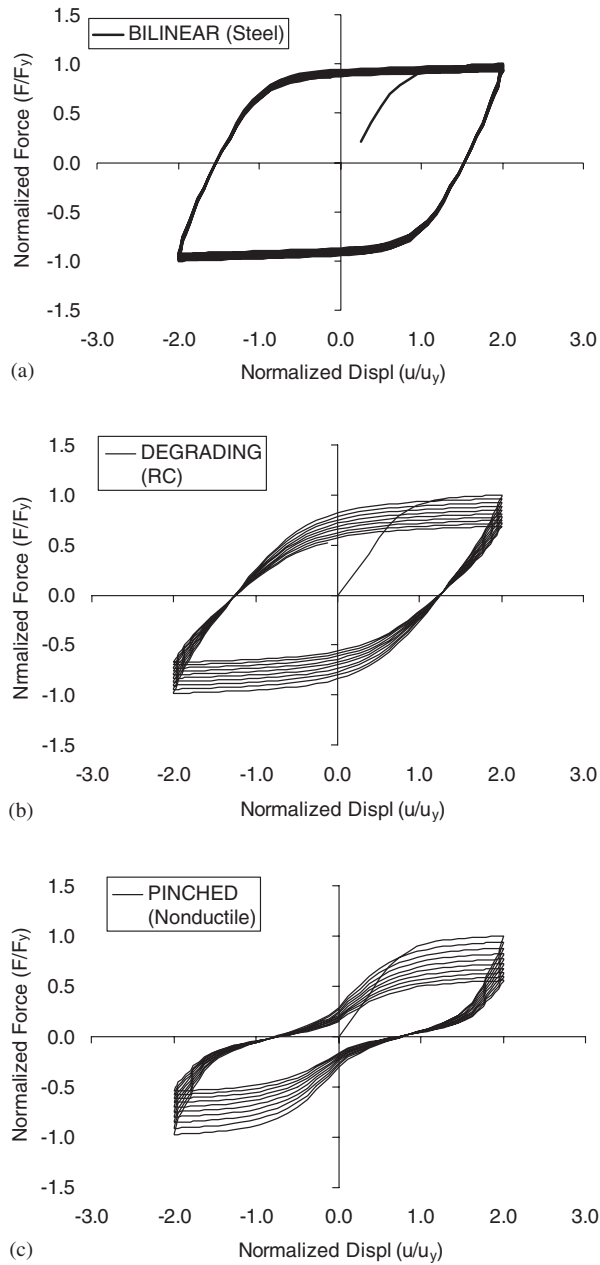


Figure 5. Hysteretic models considered: (a) bilinear behavior; (b) moderately degrading behavior (ductile RC components); and (c) severely degrading behavior.

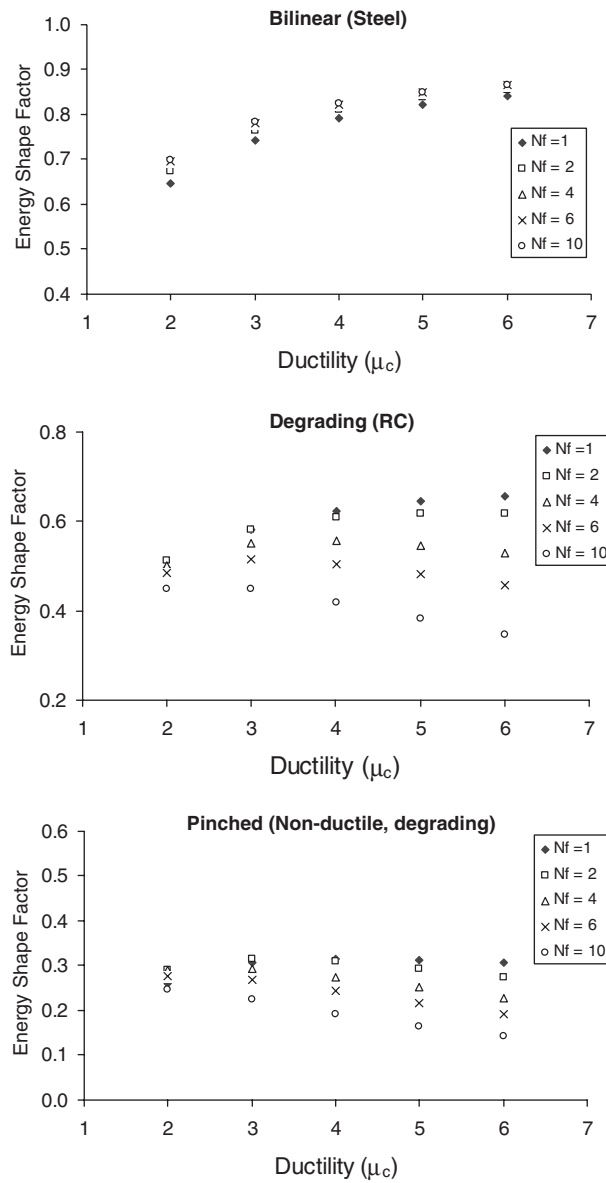


Figure 6. Calibration of hysteretic energy shape factor (α_h).

to a single-degree-of-freedom approximation. The choice of the model and material type was motivated by available low-cycle fatigue data [15] on well-detailed reinforced concrete bridge columns. The results of the low-cycle fatigue tests were recast into the following format:

$$2N_f = \left(\frac{8.25}{\mu_c} \right)^4 \tag{23}$$

where μ_c is the cyclic displacement ductility factor as defined in the derivation of the cyclic demand relation of Equation (9). It is important to point out that the above equation is valid only for seismically detailed flexurally-dominant reinforced concrete bridge columns with circular cross-section and spiral hoops. The end conditions can vary, however, the displacement used to calculate ductility should be based on tangential drift. For example, the tangential drift for a cantilever column is simply the displacement at the deck level, however, the tangential drift of a column that is part of a multi-column bent with fixed ends (moment connections) should be estimated at the contraflexure point. Additional details on the applicability of Equation (23) can be ascertained by reviewing the test set-up for the specimens used in the experiments reported by El-Bahy *et al.* [15]. Finally, it should also be noted that the use of the specific fatigue-life expression above is only meant to facilitate the validation exercise being reported in this section. If the validation were to be carried out on a different material (such as steel) or different type of structural system (such as a shear-critical column), it will be necessary to use a different relationship derived from low-cycle fatigue testing of the system.

In order to use the expression given by Equation (23), it is necessary to convert the irregular displacement history resulting from a seismic response analysis to an equivalent number of constant amplitude cycles at peak displacement ductility factor. This is accomplished by considering the number of cycles which cause failure at the target ductility (μ_{tg}). Hence, if each reversal (half-cycle) represents a ductility level i then the equivalent number of cycles at the target ductility, for bridge columns characterized by the fatigue-life relationship given by Equation (23), can be expressed as follows:

$$N_f = \frac{1}{2} \sum_{i=1}^{2n} \left(\frac{\mu_i}{\mu_{tg}} \right)^4 \quad (24)$$

where n is the number of complete cycles and $2n$ is the number of reversals or half-cycles.

The validation exercise consisted of generating time-history responses of the SDOF bridge model for a range of period values (obtained by changing the deck mass) and for each of the ground motions listed in Table I. The ground motions were uniformly scaled using a trial-and-error process so as to produce a peak displacement response corresponding to a target ductility factor. Cyclic displacement ductility factors of $\mu_c = 4.0$ and 6.0 , which are commensurate with the current level of ductility assumed for the design of bridge columns, were used as the target ductility factors in the validation studies. The resulting displacement histories were converted into equivalent cycles at the target ductility factor using Equation (24). This value, referred to as the 'simulated' response under an actual earthquake at the target ductility factor was then compared to the energy-based cyclic demand 'predicted' by Equation (9). The quantities S_a , R_μ and E_h have been defined in Equations (10), (13) and (20), respectively, and have been calculated from the ground motion parameters in Table I. Based on available test data, the hysteretic behavior of the SDOF bridge model was defined in terms of $\alpha_h = 0.5$ implying moderately degrading behavior.

Comparisons of the computed and predicted cyclic demands are shown in Figure 7 for four earthquakes selected from Table I with different ground motion characteristics [Northridge 1994 (Castaic), Chile 1985 (Llolleo), Loma Prieta 1989 (Gilroy), and Mexico City 1985 (SCT)] and a target ductility factor of 4.0. Their corresponding elastic spectral acceleration for 5% viscous damping is also shown along with each validation plot. The results displayed in Figure 7 indicate that the equivalent number of deformation cycles predicted by the cumulative

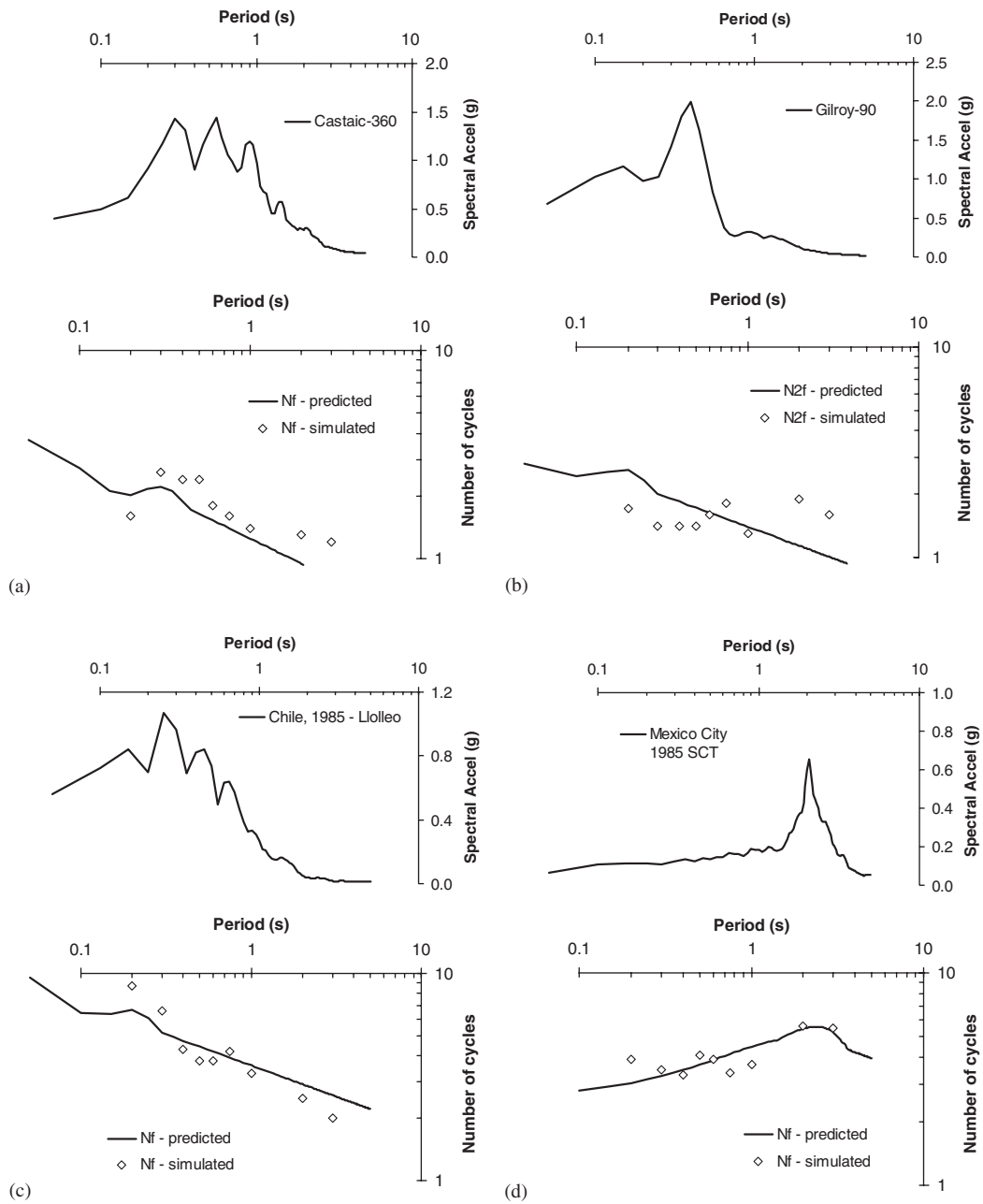


Figure 7. Validation of proposed methodology: comparison of predicted vs. simulated equivalent number of cycles at a fixed ductility of 4.0.

energy-based expression of Equation (9) is reasonable compared to the equivalent number of cycles determined from the actual number of displacement cycles (Equation (24)). For the earthquakes shown in Figure 7, the number of cycles N_f varies between 1 and 9 for a target displacement ductility factor of 4. The largest cyclic demands were imposed by the Chile and Mexico City quakes while the smallest demands came from the Loma Prieta and Northridge quakes. It can also be seen from Figures 7(a)–(d) that the predicted demand (equivalent cycles at the target ductility) is reasonably close to the actual demand computed from the response history analyses for a wide period range $0.1 < T < 3.0$. For the Castaic (Figure 7(a)) and Lollole (Figure 7(b)) ground motions, the equivalent number of load cycles generally decreases with period especially in the long-period range. For the Gilroy ground motion (Figure 7(c)) the cyclic demands are almost constant across the entire period range, probably due to the presence of a velocity pulse which typically imposes a single predominant peak cycle. For the 1985 Mexico City SCT record, the equivalent number of load cycles shows an increasing trend for periods up to 2.0 seconds due to the long-period characteristics of the ground motion as a result of soft soil conditions. Although only a subset of the validation results is shown and some scatter of data is noted, these results nonetheless demonstrate that the simplified methodology proposed to predict the cyclic demand is reasonable for preliminary design purposes.

CYCLIC DEMAND SPECTRA

The methodology represented by Equations (9) to (21) was implemented in a computer program so that a variety of demand curves could be generated for a range of ground motion parameters. Of primary interest in performance-based seismic design is the role of certain control parameters in altering the imposed cyclic demand. Since current seismic design is based on reducing elastic forces by a reduction factor, a primary variable used in the parameter study is R_μ , which is directly represented by the cyclic ductility factor μ_c . The following aspects of earthquake characteristics and system response were then investigated: the duration of the ground motion, which typically translates into increased energy demand and hence an increase in the number of load cycles, and the effects of changing the nature of the non-linear force–deformation response, which, in the present study, is represented by the three behavior patterns shown in Figure 5. In all cases, the design variable considered is the fundamental period of the structure.

Effects of degrading behavior

In this section, the effects of variation in the force–deformation behavior of the system are investigated. As the area enclosed by the hysteretic loops during a non-linear response represents the amount of irrecoverable energy dissipated by the structure, any change in the shape of the hysteretic loops is expected to influence the equivalent number of load cycles. The results presented here are based on the following ground motion parameters: duration of strong ground motion, $t_d = 20$ seconds; $\ddot{x}_{g,\max} = 0.4g$ and $\dot{x}_{g,\max} = 40$ cm/sec. These ground motion parameters corresponds to an a/v ratio of 1.0 g/ms^{-1} with a characteristic period of $T_c = 0.5$ second.

Figure 8 illustrates the change in the equivalent number of inelastic cycles as a function of cyclic ductility factor from $\mu_c = 2$ to 6, which is a reasonable range of ductility factor

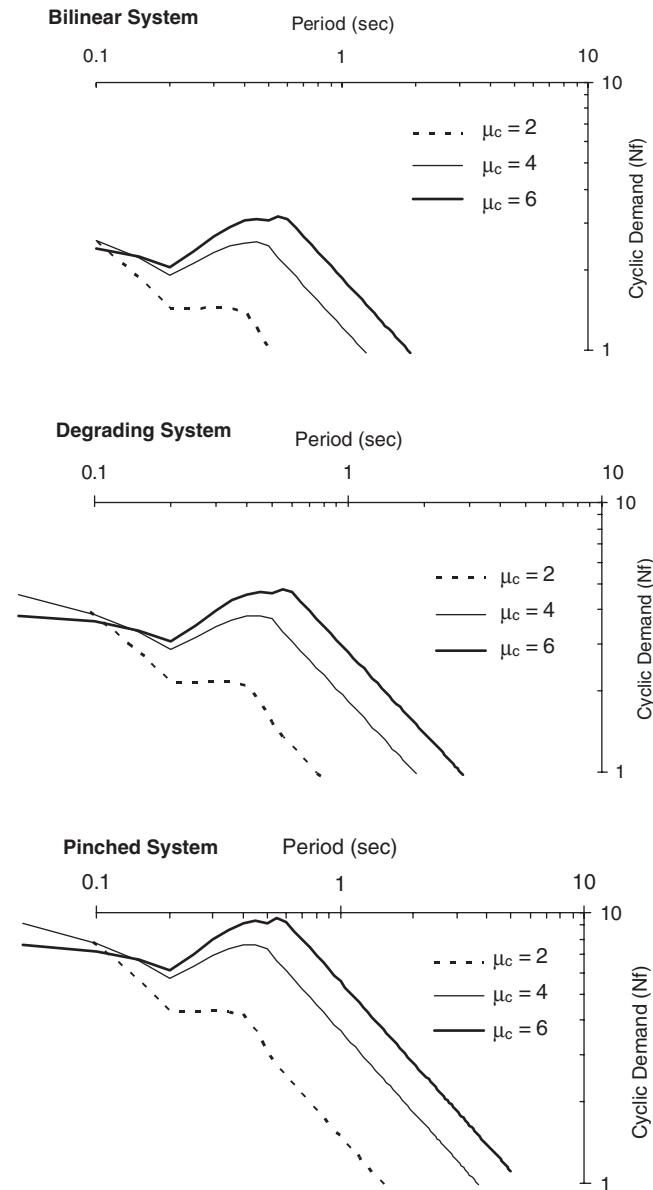


Figure 8. Effect of design ductility on energy-based cyclic demand ($t_d = 20$ seconds; $\dot{x}_{g,\max} = 0.4 g$ and $\dot{x}_{g,\max} = 40$ cm/sec).

implicit in current seismic design. A larger value of the ductility factor, μ_c , implies the use of a higher force-reduction factor R_μ and hence system yielding is initiated earlier for the same period and level of elastic force. The larger ductility factor also implies greater hysteretic energy dissipation, and consequently, low lateral strength systems (as characterized by higher

force-reduction factors or a larger ductility factor) will be subjected to an increased number of inelastic cycles. This is evident in all the plots shown in Figure 8. Additionally, the effects of moderate to severe degradation are also discernible in these figures.

For the selected ground motion parameters in Figure 8, it is observed that the cyclic demand is significantly altered for degrading and pinched systems. For very stiff systems ($0.1 \text{ s} < T < 0.2 \text{ s}$), the equivalent cyclic demands are highest and relatively independent of the ductility demand. The equivalent number of cycles increases by a factor of two when comparing bilinear force–deformation versus moderately degrading behavior and by a factor of three when the force–deformation response is pinched and severely degrading. The proposed energy-based cyclic demand parameter exhibits a local peak between 0.2 second and the characteristic period of the earthquake in all cases. In general, at periods beyond the characteristic period, the number of equivalent cycles at the target ductility begins to decrease. It should be noted that cyclic demands less than unity imply that the response is dominated by a single peak value only. Hence the cyclic demands for certain period values are not shown since the cut-off number of cycles for the target ductility was set at unity.

Effects of ground motion characteristics

Site effects. In this study, site effects are characterized by the parameter a/v which expresses the ratio of peak ground acceleration to peak ground velocity. As indicated earlier in this paper, a low a/v ratio is known to characterize a soft-soil site while a high a/v ratio characterizes a firm or rock-soil site. As illustrated previously in Figure 2, the influence of soil type is reflected not in the amplitude but in the spectral shape.

Three a/v ratios are considered in this parametric study. Figure 9 demonstrates the effectiveness of the proposed methodology to capture the influence of site effects on cyclic demand. These plots are generated for a peak ground acceleration of $0.4 g$ and peak ground velocity of 40 cm/s . The corresponding characteristic periods are indicated in the figures. For low a/v values the maximum cyclic demand is smaller than for earthquakes with a higher a/v value. In general, the demands increase from $T = 0.1 \text{ s}$ to the characteristic period T_c beyond which the demands decrease with increasing period.

An interesting observation here is the fact that the cyclic demands are higher in the low-period range for smaller ductility values (when the a/v value is low) than for larger ductilities. This is a consequence of the large characteristic period which plays an important role in determining the hysteretic energy per unit mass. For very soft soil conditions (as is the case for $a/v = 0.5 \text{ g/ms}^{-1}$), the variation of E_h/m is more abrupt, particularly for low ductility values, and though the effect appears to be pronounced in the short-period range, the change in the number of cycles is not particularly significant.

Duration effects. Another important parameter influencing the imposed demands on a structural system is the strong motion duration of the earthquake. The duration of the ground motion is defined in Equations (18a–b). Duration effects are incorporated into the present methodology through the equivalent input energy velocity, v_e (Equations (16)–(19)). The following ground motion parameters are used: $\ddot{x}_{g,\max} = 0.4g$ and $\dot{x}_{g,\max} = 40 \text{ cm/sec}$ to study the effects of ground motion duration on the number of inelastic cycles. The influence of duration is clearly evident in the plots shown in Figure 10. As expected, the equivalent number of inelastic cycles increases with increased duration of the ground motion. A larger amount

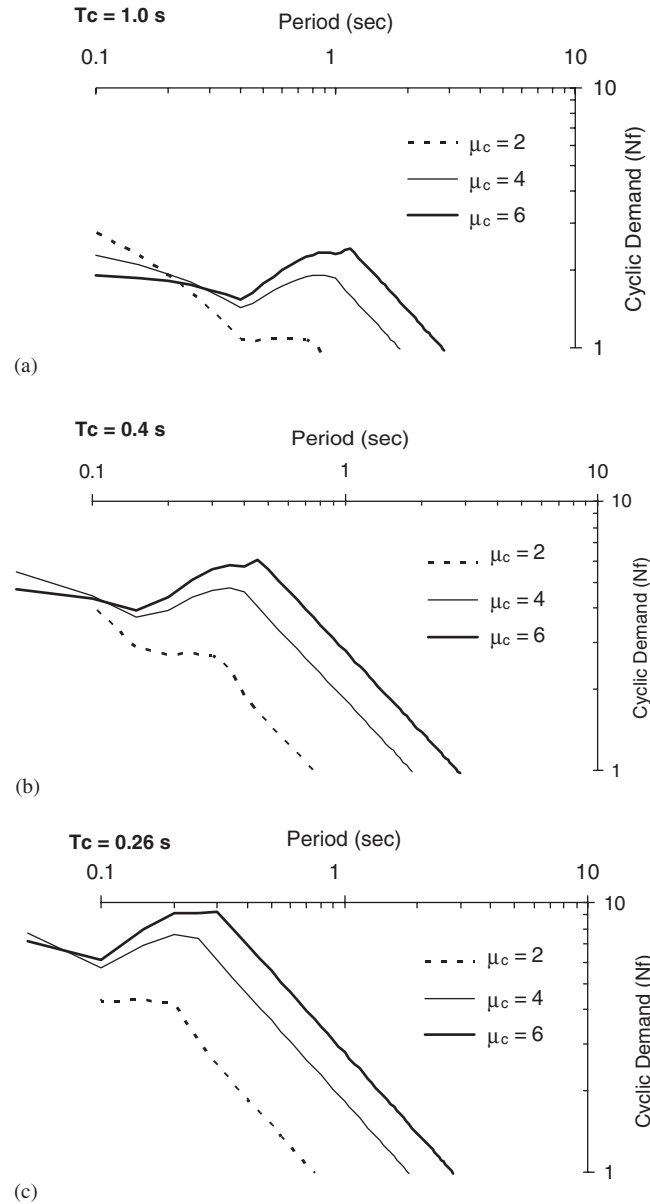


Figure 9. Effect of ground motion characteristics on energy-based cyclic demand for moderately degrading systems: $t_d = 20$ seconds and (a) $a/v = 0.5 \text{ g/ms}^{-1}$; (b) $a/v = 1.25 \text{ g/ms}^{-1}$; and (c) $a/v = 2.0 \text{ g/ms}^{-1}$.

of energy will be imparted to the structure as a result of increased ground motion duration, and the increase in input energy is reflected in the increased number of inelastic cycles. For example, at a target ductility demand of 4.0, for an increase in duration from $t_d = 10$ seconds to 30 seconds, the equivalent number of cycles increases from approximately 2.0 to 6.0 for

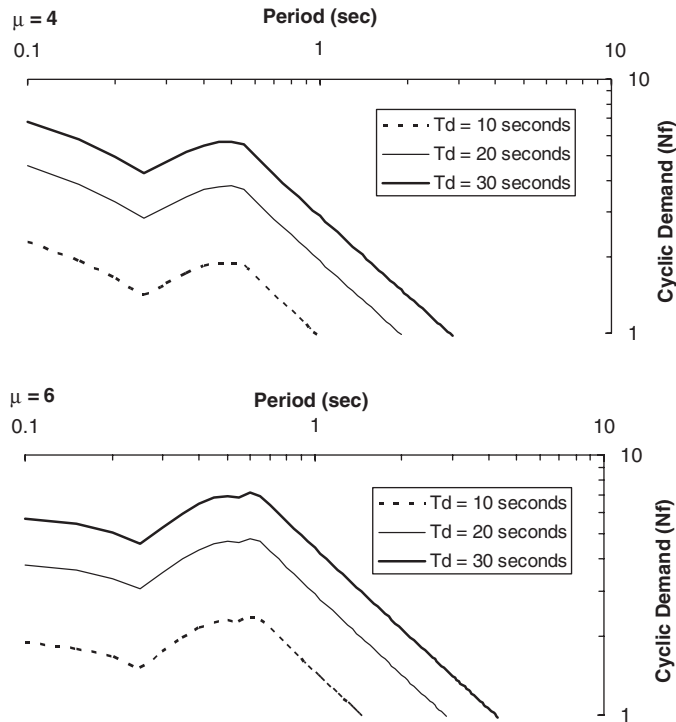


Figure 10. Effect of duration on energy-based cyclic demand for moderately degrading systems ($\dot{x}_{g,max} = 0.4 g$ and $\dot{x}_{g,max} = 40 \text{ cm/sec}$) $T_c = 0.5 \text{ s}$.

a period of $T = 0.5$ second. By comparing the two different plots in Figure 10, it can be seen that the equivalent number of cycles increases with increasing yielding of the structure as characterized by the increase in the cyclic displacement ductility factor from $\mu_c = 4$ to 6. For a given duration, a larger amount of energy is dissipated by the structure leading to an increased displacement ductility demand, and hence a larger number of cycles.

The plots represented by Figures 8–10 are influenced by the choice of the critical design parameters that appear in Equation (9). In the present study, these parameters were based on empirical values defined in Equations (10)–(21). The variations observed in some of these plots, particularly in the short-period range, are sensitive to the choice of these parameters. Hence, no attempt is made to attach any significance to these anomalies. The general trends represented by the figures point to the influence of cumulative effects on cyclic demand which is the primary theme of this paper.

DESIGN PROCEDURE WITH EXAMPLE

The proposed methodology is best used as an evaluation tool after a traditional seismic design to estimate the number of inelastic cycles to be expected at the target ductility. It can be

incorporated into any iterative design process. A typical step-by-step procedure is described below

1. Given the ground motion parameters PGA, PGV and strong motion duration, complete a preliminary design using trial member sizes and assumed section details.
2. Estimate the fundamental period of the structure using the preliminary configuration and known structural mass (m).
3. Estimate S_a from Equation (10). For the desired ductility, estimate the force-reduction factor R_μ using Equation (13). Compute the elastic base shear $V_e = mS_a$ and the yield strength of the structure $V_y = V_e/R_\mu$. This establishes the yield displacement (V_y/k_o) where k_o is the initial stiffness of the structure.
4. Size the members to achieve the yield strength of the structure and calculate the actual yield displacement. For a SDOF structure this is accomplished easily, however, for a MDOF structure, an approximate plastic analysis or non-linear static analysis must be performed to estimate this quantity.
5. An iterative approach is used until the achieved ductility matches the target ductility.
6. Estimate the hysteretic energy per unit mass using Equation (20). For the given structural system, assume a value of the energy shape factor α_h using the guidelines recommended in the paper (Figure 5).
7. Calculate the inelastic cyclic demand using Equation (9).

Alternatively, if a displacement-based or code approach is used to design the structure, the estimation of cyclic demand requires the calculation of S_a (Equation (10)), R_μ (Equation (13)), and E_h/m (Equation (20)).

Illustrative example

The basic design parameters for this example are taken from Chopra and Goel [16] wherein the authors illustrate the design of a bridge column using a direct displacement method in conjunction with an inelastic spectrum. A reinforced concrete column 4 m high is part of a long viaduct and supports a total mass of 767 041 kg. Since the pier and the tributary area of the deck it supports can be represented by a single-degree-of-freedom system, the cyclic demand imposed on the column is amenable to the proposed methodology in a relatively direct manner. The column is assumed to have a diameter of 1.5 m and a concrete compressive strength of 27.6 MPa. The elastic modulus based on the ACI 318 [17] provisions is 24 850 MPa. This results in an initial lateral stiffness of 1512 kN/cm and a fundamental period of 0.45 sec. In the direct displacement methodology proposed by Chopra and Goel, the design earthquake has a peak ground acceleration of 0.5 g and a corresponding peak ground velocity of 0.61 m/sec. Using Equations (9)–(21), the following intermediate parameters are obtained: a characteristic period $T_c = 0.63$ sec; a transition period $T_o = 0.69$ sec; $R_\mu = 4.1$; $\Omega_v = 3.8$ and $E_h/m = 1.86$ m/s². For a target ductility of 5.8 (used by Chopra and Goel in their example), an assumed energy shape factor of 0.5 and strong motion duration of 20 seconds, the cyclic demand is estimated as 3.6 (Equation (9)). The resulting elastic base shear is 9396 kN and the corresponding yield shear to achieve a reduction factor of 4.1 is 2282 kN. This translates into a yield displacement of 1.51 cm and a maximum displacement of 8.76 cm. This constitutes the preliminary design. An iterative approach must now be used to accomplish the objective outlined in Step 5. For example, in the direct displacement design methodology proposed by Chopra and

Goel, the iterative process resulted in a yield displacement of 1.67 and a peak displacement of 9.7 cm.

The main advantage of the proposed methodology is its ability to examine the effects of parameters that influence cyclic demand. In the above example it is established that the bridge column will need to sustain 3.6 cycles at a peak displacement of 8.76 cm. If the ductility demand or the number of cycles at the specified demand needs to be reduced, yielding must be delayed or the strength of the section must be increased. Additionally, any increase in the duration of the strong motion will increase cyclic demand. For example, if the strong motion duration is increased from 20 to 30 seconds, the cyclic demand increases to 5.2. Likewise, if the stiffness is increased to 2000 kN/m and the period drops to 0.39 seconds, the cyclic demand is reduced to 3.3 and the yield shear increases to 2533 kN.

Ultimately, it must be reiterated that the above example is meant to illustrate the utility and advantages of the methodology rather than claim to offer a better prediction of seismic demand. As suggested earlier in this paper, the empirical relationships used in the formulation can be substituted with improved expressions as additional calibration studies become available.

FINDINGS, CONCLUSIONS AND LIMITATIONS

The proposed formulation for developing a demand spectrum incorporates standard seismic design criteria such as force-reduction factors and an acceleration design spectrum thereby enabling a clearer understanding of the implications of design choices on inelastic cyclic demand. Results of the study indicate that cumulative effects are dependent on the characteristic period of the earthquake with peak cyclic demands occurring in the region of the characteristic period value. Cumulative effects are less significant for long-period structures, viz., those with periods much larger than the characteristic period. The demands are sensitive to site effects, ground motion duration and the force–deformation characteristics of the structural system. In general, it is observed that the deformation demands imposed by an earthquake on a structure consist of more than one equivalent cycle at the target ductility. For earthquakes with strong motion duration of about 30 seconds and a target ductility of 6.0, the study shows that the cyclic demand can be as high as 6 to 8 full cycles at the design ductility for structures in the period range from 0.1–1.0 seconds. The ability of structural components to withstand cyclic loads at the design ductility is only implied in modern codes through detailing criteria which control strength degradation due to repeated cycling. However, no explicit criteria exist to define or quantify the number of cycles at a specified ductility. Some of the results presented in this paper shed some light on this subject and the general methodology proposed is expected to contribute to ongoing efforts that incorporate inelastic cyclic effects in the design process.

In the present formulation, it was implicitly assumed that structural systems can be reasonably represented by equivalent SDOF models. Hence the equations derived in this paper are generally valid for those systems that have a predominant first-mode behavior. Additional studies are needed to investigate the influence of multi-mode response and more realistic deformation measures such as inter-story drift. However, the approach and concepts presented in this paper can be extended to more general systems. Studies are underway to examine other relevant cyclic response quantities such as inter-story drift since the drift response is more indicative of local member demands in multistory buildings. Other issues related to ground motion characteristics, such as velocity pulses and near-source effects, also need to be addressed.

ACKNOWLEDGEMENTS

This study is part of a more comprehensive project supported by the National Science Foundation under Grant CMS-0296210, as part of the US–Japan Cooperative Program on Urban Earthquake Disaster Mitigation. Any opinions, findings, and conclusions or recommendations expressed in this material are those of the authors and do not necessarily reflect the views of the National Science Foundation.

REFERENCES

1. Malhotra PK. Cyclic-demand spectrum. *Earthquake Engineering and Structural Dynamics* 2002; **31**:1441–1457.
2. Uang C-M, Bertero VV. Evaluation of seismic energy in structures. *Earthquake Engineering and Structural Dynamics* 1990; **19**:77–90.
3. Fajfar P, Vidic T. Consistent inelastic design spectra: hysteretic and input energy. *Earthquake Engineering and Structural Dynamics* 1994; **23**:523–538.
4. Manfredi G. Evaluation of seismic energy demand. *Earthquake Engineering and Structural Dynamics* 2001; **30**:485–499.
5. Kuwamura H, Kirino Y, Akiyama H. Prediction of earthquake energy input from smoothed Fourier amplitude spectrum. *Earthquake Engineering and Structural Dynamics* 1994; **23**:1125–1137.
6. Chai YH, Fajfar P. A procedure for estimating input energy spectra for seismic design. *Journal of Earthquake Engineering* 2000; **4**(4):539–561.
7. Vidic T, Fajfar P, Fischinger M. Consistent inelastic design spectra: strength and displacement. *Earthquake Engineering and Structural Dynamics* 1994; **23**:507–521.
8. Chai YH, Fajfar P, Romstad K. Formulation of duration-dependent inelastic seismic design spectrum. *Journal of Structural Engineering* (ASCE) 1998; **124**(8):913–921.
9. Trifunac MD, Brady AG. A study on the duration of strong earthquake ground motion. *Bulletin of the Seismological Society of America* 1975; **65**:581–626.
10. Baber TT, Noori MN. Random vibration of degrading, pinching systems. *Journal of Engineering Mechanics* (ASCE) 1985; **111**(8):1010–1026.
11. Kunnath SK, Mander JB, Fang L. Parameter identification for degrading and pinched hysteretic structural concrete systems. *Engineering Structures* 1997; **19**(3):224–232.
12. Coffin LF Jr. A study of the effect of cyclic thermal stresses in ductile metals. *Transactions of the ASME* 1954; **76**:931–950.
13. Manson SS. Behavior of materials under conditions of thermal stress. *Heat Transfer Symposium*. University of Michigan 1953: 9–75.
14. Miner MA. Cumulative damage in fatigue. *Journal of Applied Mechanics* (ASME) 1945; **12**:159–164.
15. El-Bahy A, Kunnath SK, Stone WC, Taylor AW. Cumulative seismic damage of circular bridge columns: benchmark and low-cycle fatigue tests. *ACI Structural Journal* 1999; **96**(4):633–641.
16. Chopra A, Goel R. Direct displacement-based design: use of inelastic vs. elastic design spectra. *Earthquake Spectra* 2001; **17**(1):47–64.
17. ACI-318. Building Code Requirements for Structural Concrete, American Concrete Institute, Farmington Hills, MI, 2002.